Creating and probing subwavelength atomic gratings using spatially separated fields

B. Dubetsky and P. R. Berman
Physics Department, University of Michigan, Randall Laboratories, Ann Arbor, Michigan 48109-1120
(Received 31 March 1994)

The interaction of an atomic beam with three spatially separated linearly polarized standing-wave fields is considered, taking into account the magnetic degeneracy and hyperfine splitting of the atomic levels. A spatial modulation of the ground-state density matrix occurs, and is not washed out as a result of spontaneous decay from the upper states. The interaction with fields separated by a distance L results in a focusing of harmonics at distances $L'=(m/n)L$, where m and n are integers; the period of the matter gratings is $\lambda/2n$, where λ is the wavelength of the radiation field. For a beam having angular divergence θ, one can observe these higher harmonics independently from each other if $L \gg \lambda/\theta$. The gratings can be probed using a third standing-wave laser field in the focal plane of the harmonic under investigation. General expressions that allow one to calculate the probe absorption for atoms having arbitrary fine and hyperfine structure are derived. Explicit calculations for the alkali metals are presented. It is predicted that spatial modulations having periods 30–500 nm and modulation depths 2.5–50 % can be produced in this manner. The focusing of the spatial harmonics is interpreted in terms of a shadow effect.

PACS number(s): 03.75.Dg, 32.80.Wr, 42.50.Hz, 42.50.Vk

I. INTRODUCTION

The spatial degrees of freedom of neutral atoms can be modified by allowing the atoms to interact with resonant optical fields. The use of counterpropagating waves allows one to cool atoms below the Doppler limit of laser cooling [1], construct atom matter-wave interferometers [2–5], focus an atomic beam [6–8], etc. At the heart of these phenomena is the atomic recoil accompanying the absorption or emission of the resonant radiation. To describe the recoil process, one needs an entirely quantum treatment of the atomic spatial motion.

There are, however, other means for optically manipulating the atoms' spatial degrees of freedom which do not relay on atomic recoil for their existence. For instance, interaction with a resonant standing-wave field results in spatial modulation of the atomic levels' populations with periods equal to $\lambda/2s$, where λ is the optical wavelength and s is an integer greater than 0. These higher harmonics of the atomic density could, in principle, be deposited on a solid surface to form diffraction gratings having spacings of order 10–100 nm. Unfortunately, all the gratings are superposed and some method for separation of the individual gratings is needed.

The shadow effect, proposed earlier [3], allows one to achieve this goal. The action of a standing wave on a given level population can be simulated qualitatively by the action of a grating with period $\lambda/2$. Consider the passage of an atomic beam through the grating (see Fig. 1). The beam is spatially modulated just after passage through the grating, but this modulation is destroyed rapidly as a result of atomic motion. Indeed, for an atomic beam having angular divergence θ, the transverse atomic motion results in a washing out of the grating in a longitudinal distance of order λ/θ. This decay of the spatial modulation is similar to that observed in the free induction decay of an inhomogeneously broadened atomic ensemble excited by a resonant pulse. The decay is not irreversible, however, and the spatial modulation can be restored using echo techniques. Superposition of the two shadows created by the atomic beam passing through two gratings separated from each other by a distance $L \gg \lambda/\theta$ results in the recovering of the spatial harmonic at the distance $2L$ (see Fig. 1).

To demonstrate this shadow effect one can use incoherent light [9] instead of an atomic beam. By passing

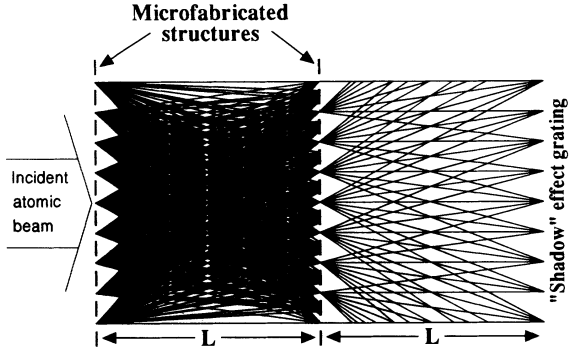

FIG. 1. "Shadow" effect. Microfabricated structures with period d simulate action of separated standing waves with wavelength $\lambda=2d$. An atomic density grating, i.e., a periodical spatial distribution with period $\lambda/2$, appears just after the first structure. Overlapping of the trajectories of atoms passing through the different slits results in the rapid destruction of the grating in a distance λ/θ. An atomic beam with angular divergence $\theta \sim 1$ is assumed here. The trajectories of the particles passing through the centers of slits are shown after the second microfabricated structure. Superposition of the "shadows" from the first and second structures leads to grating reconstruction exactly at the distance $2L$.

light through spatially separated gratings, one observes a spatial modulation of the light intensity similar to that shown in Fig. 1. The use of gratings having variable periods allows one to observe the harmonics in different focal planes [10]. If microfabricated gratings [11] having variable period are used, an analogous effect will occur for an atomic beam having large angular divergence. We consider only gratings have equal periods in this paper.

As is evident from Fig. 2, harmonics other than the second can also be produced, the fourth harmonic at distance $L'=\frac{3}{2}L$, the sixth at distance $L'=\frac{4}{3}L$, and so on. Thus, the "interaction" with two gratings results in a spatial separation of the focal planes of the different harmonics. The "rephasing" of the spatial modulation in space is analogous to the rephasing of atomic dipoles in time to produce a photon echo.

The separation of the higher-order gratings also occurs under the action of resonant standing-wave fields. One can conclude from Fig. 2 that higher harmonics are focused at all distances L' such that the ratio L'/L is rational, i.e.,

$$L'/L=m/n \tag{1}$$

where m and n are integers. Localization of the higher harmonics of the density matrix was predicted in [12] for temporally separated standing-wave fields. There is no physical difference between time- and space-separated fields since, in the atomic rest frame, fields separated by distance L appear as pulses delayed in time by $T=L/u$, where u is the atomic velocity. Backward scattering of a probe traveling-wave pulse was used to monitor the second harmonic of the levels populations localized at the time $T'=\frac{3}{2}T$ [12]. This method is inappropriate for probing harmonics with period less than $\lambda/2$. To probe the higher-order gratings one can use a third, strong standing-wave field [13]. Interaction with the strong field, applied at the point of localization of the grating with period $\lambda/2s$ (i.e., harmonic $2s$), results in an absorption signal from which information concerning the spatial modulation of the medium can be extracted.

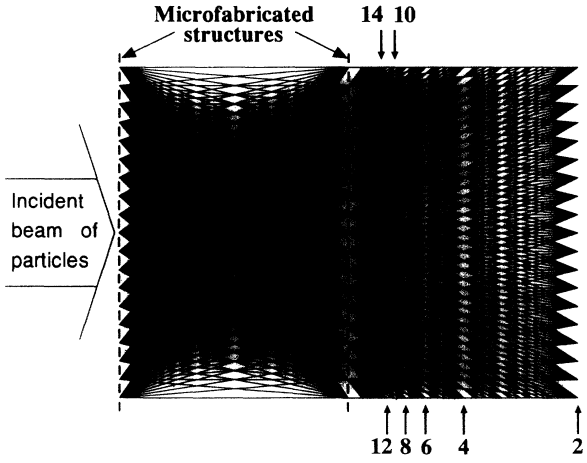

FIG. 2. "Shadow" effect using two microfabricated structures of 20 slits each; n th arrow shows point of localization for harmonic n. The gratings appearing at distance between the structures are washed out by trajectories (not shown) which do not pass through the second set of slits.

The shadow effect was considered previously for a weak forbidden transition [12,13] and for an allowed transition in which the probability of radiative decay from the upper to lower level was negligible [3]. An important class of optical transitions, strong transitions between ground and first excited states, necessitates a different analysis. The decay between levels plays such an essential role in this case that the two-level model, used previously, becomes inapplicable. For the two-level model, the ground-state gratings vanish, canceled by the combined action of stimulated processes and spontaneous decay [14]. When the magnetic degeneracy of the levels as well as their hyperfine structure is included, however, one finds that it is possible to generate nonvanishing ground-state gratings. The physical origin of this effect is discussed in detail in Refs. [14–17].

It is necessary to underline the fact that the shadow effect occurs at the same echo points as matter-wave interference. In any interference experiments both phenomena play a role. One may want to distinguish the entirely quantum matter-wave interference from the entirely classical shadow effect. Since the sum of populations (atomic beam density f) is conserved for each velocity subgroup for particles moving classically, no spatial harmonic of the total density can be induced [15]. The gratings of the density f appear only after taking into account the recoil effect for situations in which time of flight between fields becomes comparable with the inverse recoil frequency $\omega_k^{-1}=(\hbar k^2/2M)^{-1}$, where M is atomic mass. It was proved previously [2,3] that, however, no gratings of density can be observed on an allowed transition exactly at the echo point. This result can be generalized to the case of multilevel atoms. To observe the matter-wave interference, one has to consider the signal in the vicinity of the echo points, where nonvanishing gratings of the total density appear following strong saturation of the transition by the first standing-wave field [2,3].

Even though we consider the shadow effect as arising from motion along classical trajectories, observable modifications of the shadow effect can result from phenomena related to quantization of the atomic motion. Such effects result in recoil splitting of the Lamb dip [18,19] and Ramsey fringes [20–22], and are responsible for the appearance of recoil-induced resonances in pump-probe spectroscopy and four-wave mixing [23,24]. For the shadow effect, the same process leads to an oscillating dependence of the amplitudes of the atomic gratings as a function of the time $T=L/u$, with a period of order of the inverse recoil frequency ω_k^{-1}. Observation of this oscillation permits one to measure ω_k on an allowed transition without a need for high-frequency resolution.

We plan to analyze the interplay of the shadow effect and matter-wave interference in the future. In this paper, it is assumed that $\omega_k T \ll 1$, consequently effects related to quantization of the atoms' center-of-mass motion can be ignored. Note that the condition $\omega_k T \ll 1$ can be rewritten as $(\hbar k/M)T \ll k^{-1}=\lambda/2\pi$, implying that atomic recoil on the absorption or emission of radiation is negligible if $\omega_k T \ll 1$.

An atomic beam interacts with three, spatially separated standing-wave fields resonant on an allowed transition. We assume that the excited-state lifetime of the atoms is smaller than the time of interaction with each field. It is then possible to adiabatically eliminate the ground-excited state optical coherence and excited-state populations and use rate equations for the multilevel, ground-state density matrix elements [25]. In Sec. II these equations are solved for linearly polarized standing waves and general expressions for absorption by the third field are obtained. Section III is devoted to a discussion of the results. It is shown that it is possible to create high-order spatial gratings using low to moderate laser power. Specific values for the optimum field powers are given for the alkali-metal elements.

II. SIGNAL CALCULATION

A schematic picture of the system under consideration is shown in Fig. 3. An atomic beam having angular divergence θ passes through three standing-wave optical fields. The absorption of the third field is monitored as a function of the fields' powers, frequencies and phases.

The electric-field vector of the linearly polarized standing waves is taken as

$$\begin{aligned}\mathbf{E}(\mathbf{r},t)&=\sum_{j=1}^{3}\mathbf{E}_j(\mathbf{r},t)\ ,\\ \mathbf{E}_j(\mathbf{r},t)&=\epsilon E_j f(x-L_j,y)\\ &\quad\times\cos(\mathbf{kz}+\varphi_j)\exp(-i\Omega t)+\text{c.c.},\end{aligned}\tag{2}$$

where Ω, k, and ϵ are the frequency, propagation constant and unit polarization vector of the field. Field j has amplitude E_j, spatial phase φ_j, and is centered at $x=L_j$, $y=0$, where $L_1=0$, $L_2=L$, $L_3=L'$. The function $f(x,y)$ specifies the transverse spatial profile of the field; it is centered at $(x,y)=(0,0)$ and has apertures w_x and w_y in the x and y directions, respectively.

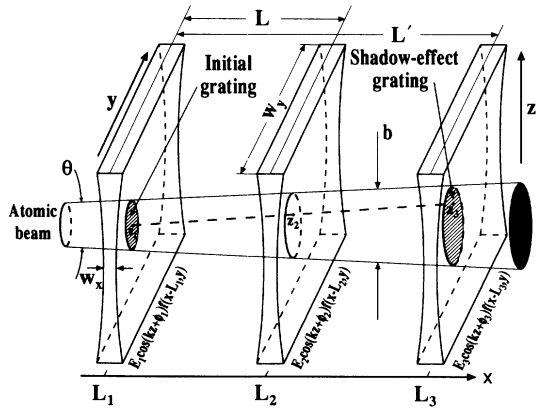

FIG. 3. Schematic diagram of the problem under consideration. An atomic beam having angular divergence θ and aperture b propagates along the x axis and is illuminated by three resonant, spatially separated standing-wave fields, which propagate along the z direction and have different apertures $w_x \ll \lambda/\theta$ and $w_y \gg b$. The first field induces a spatial modulation of the beam which dephases rapidly for the ensemble, the second-field starts the rephasing process and the third field probes the higher-order harmonic focused at the distance L'. A trajectory of atom passing through the field zones at the points having z coordinates z_1, z_2, z_3 is shown.

Atomic ground and excited states, having electronic angular momenta J and J', respectively, are split into hyperfine sublevels having total angular momenta $|J-I| \le G \le J+I$ and $|J'-I| \le H \le J'+I$, where I is the nuclear spin. We assume that the hyperfine splitting is resolved so that field (2) is resonant with a particular $G \rightarrow H$ transition. It is furthermore assumed that duration of the interaction with each field, $\tau = w_x/u$, is sufficiently large to ensure that

$$\tau \max\{\Gamma, |\Delta|\} \gg 1\ ,\tag{3}$$

where Γ^{-1} is an excited state lifetime and $\Delta=\Omega-\omega_{HG}$ is an atom-field detuning, and that the incident fields are sufficiently weak to ensure that the Rabi frequencies χ_j satisfy

$$\chi_j = p_{J'J}E_j/(2\sqrt{3}\hbar) \ll \Gamma\ ,\tag{4}$$

where $p_{J'J}$ is the reduced matrix element of the dipole moment operator between states J' and J.

Under these assumptions, one can use equations for ground-state density-matrix elements derived in [25] (see also [26]) in which terms involving the excited states have been adiabatically eliminated. It is convenient to expand the density-matrix elements in an irreducible tensor basis, defined by

$$\begin{aligned}\bar{\rho}_Q^K(G,G')&=(-1)^{G-m}\{K\}\begin{bmatrix}G & G' & K\\ m & -m & -Q\end{bmatrix}\\ &\quad\times\langle G,m|\rho|G',m'\rangle\ ,\end{aligned}\tag{5}$$

where

$$\{X_1^{(n_1)}\cdots X_s^{(n_s)}\}=[(2X_1+1)^{n_1}\cdots(2X_s+1)^{n_s}]^{1/2}\ ,\tag{6}$$

and $\begin{bmatrix}\cdots\\ \cdots\end{bmatrix}$ is a 3-J symbol. A summation convention is used in Eq. (5) and all subsequent equations in which repeated indices and symbols appearing on the rhs (right-hand side) of an equation are to be summed over, *except* if they also appear on lhs (left-hand side) of the equation. Ground-state coherence between different hyperfine levels can be neglected on the assumption that the hyperfine intervals of the ground and excited states satisfy $|\omega_{GG'}| \gg \Gamma$ $(G \neq G')$ and $|\omega_{HH'}| \gg \Gamma$ $(H \neq H')$ and, that for any G, G', H, H', $|\omega_{GG'}-\omega_{HH'}| \gg \Gamma$, except if $G=G'$ and $H=H'$.

If the quantization axis is taken in the direction of the polarization vector ϵ, it follows that only those multipoles of ρ with zero magnetic quantum number Q

$$\rho_K(G) \equiv \bar{\rho}_0^K(G,G)\ ,\tag{7}$$

and created by the fields. After adiabatic elimination of the density-matrix elements involving excited states, one finds that the ground-states elements evolve as [25,26]

$$\begin{aligned}\frac{d}{dt'}\rho_K(G)&=\xi_j\{1+\cos[\mathbf{qz}(t')+2\varphi_j]\}\\ &\quad\times|\psi_j(t')|^2 R_{KK'}\rho_{K'}(G)\ ,\end{aligned}\tag{8a}$$

where

$$R_{KK'}=3(-1)^{H-G}(\delta_{\bar{K}0}\sqrt{\tfrac{1}{3}}-\delta_{\bar{K}2}\sqrt{2/3})\begin{Bmatrix}K & K' & \bar{K}\\ 0 & 0 & 0\end{Bmatrix}\{KK'\bar{K}H^2G^2\}\begin{Bmatrix}J' & H & I\\ G & J & 1\end{Bmatrix}^2$$
$$\times\left[\begin{Bmatrix}K & K' & \bar{K}\\ G & G & G\end{Bmatrix}\begin{Bmatrix}1 & 1 & \bar{K}\\ G & G & H\end{Bmatrix}-(-1)^{2G}\{G^2H^2J'^2\}\begin{Bmatrix}J' & H & I\\ G & J & I\end{Bmatrix}^2\begin{Bmatrix}H & H & K\\ G & G & 1\end{Bmatrix}\begin{Bmatrix}K & K' & \bar{K}\\ H & G & 1\\ H & G & 1\end{Bmatrix}\right], \tag{8b}$$

$$q=2k\ , \tag{8c}$$

$$\xi_j=2|\chi_j|^2\Gamma/(\gamma^2+\Delta^2)\ , \tag{8d}$$

$$\psi_j(t')=f(x(t')-L_j,0)\ , \tag{8e}$$

$\gamma=\Gamma/2$ is the homogeneous width of the $G\rightarrow H$ transition, and $\{\cdots\}$ and $\{\begin{smallmatrix}\cdots\\ \cdots\end{smallmatrix}\}$ are 6-J and 9-J symbols, respectively. Equations (8) are written in the atomic rest frame. To transform to the laboratory frame $(\mathbf{r},t)$, one sets

$$\mathbf{r}(t')=\mathbf{r}-\mathbf{u}(t-t')\ , \tag{9}$$

where $\mathbf{u}$ is an atomic velocity. For the absorption of the third field, we are interested only in those values of x satisfying

$$|x-L'|\lesssim w_x\ . \tag{10}$$

The further simplify Eqs. (8), we adopt the following additional assumptions: (1) the beam's angular divergence θ is small enough to neglect atomic motion in the y direction for the entire time of interaction, i.e.,

$$\theta L'/w_y\ll 1\ ; \tag{11}$$

(2) the field aperture w_x is sufficiently small to allow all atomic velocity subgroups to contribute to the shadow signal, i.e.,

$$kv\tau\sim ku\theta w_x/u=kw_x\theta\ll 1\ , \tag{12}$$

where v is the z component of the atomic velocity ($v\sim\theta u\ll u$); (3) the angular divergence is sufficiently large to ensure that the spatially modulated ground-state Zeeman coherence undergoes the proper dephasing-rephasing cycle associated with echo production,

$$kv(L/u)\sim L\theta/\lambda\gg 1\ ; \tag{13}$$

(4) the radial dimension b of the atomic beam is smaller than w_y and smaller than the confocal parameter w_x^2/λ (so that all atoms in the beam see the same field amplitude in each field region), but larger than the wavelength λ (so that the atoms see many spatial cycles of the field):

$$\lambda\ll b\ll\min\{w_y,w_x/\lambda^2\}\ . \tag{14}$$

Condition (12) permits one to neglect atomic motion along the z axis during each atom-field interaction. Consequently, for interaction with field j, one can set

$$z(t')=z_j=z-v(T_3-T_j)\ , \tag{15}$$

in Eq. (8), where

$$T_j=L_j/u\ . \tag{16}$$

Each location z in the final interaction region correlates with specific z components in each of the first two interaction zones as shown in Fig. 3.

The power absorbed from the third standing wave by the atomic beam is given by

$$W=\int d^3r d^3u\,\mathbf{E}(\mathbf{r},t)\cdot\partial\mathcal{P}(\mathbf{r},\mathbf{u},t)/\partial t\ , \tag{17}$$

where $\mathcal{P}(\mathbf{r},\mathbf{u},t)=[\mathcal{P}(\mathbf{r},\mathbf{u})\exp(-i\Omega t)+\text{c.c}]$. is the polarization density. The polarization density is equal to the average value of the dipole moment operator, which, in turn, is proportional to off-diagonal density-matrix elements involving ground and excited states [14]. These density-matrix elements can be reexpressed in terms of the ground-state density matrix via the adiabatic elimination procedure referred to previously [25]. As a result, the circular components of the polarization $\mathcal{P}_q$, defined by

$$\mathcal{P}(\mathbf{r},\mathbf{u})=(-1)^q\mathcal{P}_{-q}(\mathbf{r},\mathbf{u})\hat{\boldsymbol{\epsilon}}_q\ , \tag{18}$$

with

$$\hat{\epsilon}_{\pm1}=\mp(\hat{\mathbf{x}}'\pm i\hat{\mathbf{y}}')/\sqrt{2},\hat{\boldsymbol{\epsilon}}_0=\hat{\mathbf{z}}'\ , \tag{19}$$

can be written in terms of ground-state density-matrix elements as [25,26]

$$\mathcal{P}_q(\mathbf{r},\mathbf{u})=i(-1)^{H+G+K+q'}(E_3/\hbar)f(x-L',y)$$
$$\times\cos(kz+\varphi_3)|p_{HG}|^2\epsilon_{q'}(\gamma-i\Delta)^{-1}$$
$$\times\{K\}\begin{Bmatrix}1 & 1 & K\\ q & -q' & 0\end{Bmatrix}\begin{Bmatrix}1 & 1 & K\\ G & G & H\end{Bmatrix}\rho_{\mathbf{K}}(G)\ , \tag{20}$$

where ϵ_q are the circular components of the vector $\boldsymbol{\epsilon}$ expanded in the basis (19). The polarization components $\hat{\boldsymbol{\epsilon}}_q$ are defined in a coordinate system whose $\mathbf{z}'$ axis is taken along the direction of $\boldsymbol{\epsilon}$, implying that

$$\epsilon_q=\delta_{q0}\ . \tag{21}$$

Combining Eqs. (17)–(21) and assuming a monoenergetic beam with speed u, one arrives at the expression

$$W=3(-1)^{H+G'+K}\hbar\Omega NS$$
$$\times\{H^2G^2\}\begin{Bmatrix}J' & H & I\\ G & J & I\end{Bmatrix}^2\begin{Bmatrix}1 & 1 & K\\ G & G & H\end{Bmatrix}$$
$$\times\xi_3\langle[1+\cos(q\mathbf{z}+2\varphi_3)]\int_{-\infty}^{\infty}dx\,\epsilon_0^K\rho_K(G)\rangle \tag{22}$$

where

$$\epsilon_0^K=(-1)^s\{K\}\begin{bmatrix}1 & 1 & K\\ s & s' & -0\end{bmatrix}\epsilon_s(\epsilon_{-s'})^*$$

is a component of a coupled basis polarization tensor [25], N and $S\sim b^2$ are the atomic beam density and cross section, respectively, and $\langle\ \rangle$ indicates an average over v and z, which is equivalent to averaging over all atoms passing through the three-field regions. For linearly polarized fields (21), it follows that

$$\epsilon_0^K=(-\sqrt{\tfrac{1}{3}}\delta_{K0}+\sqrt{\tfrac{2}{3}}\delta_{K2})\ . \tag{23}$$

In principle, $\rho_K(G)$ can depend on t since it is a solution of Eq. (8a). To prove that there is actually no such dependence in the case of spatially separated fields, one can formally solve Eq. (8a) to obtain

$$\rho_K(G)=\left\{\exp\left[\mathbf{R}\int_{-\infty}^{t}dt'\xi_j(1+\cos\{q[z-v(t-t')]\})\times|f_j[x-u(t-t')-L_j,0]|^2\right]\right\}_{KK'}\rho^i_{K'}(G)\ , \tag{24}$$

where $\rho^i_{K'}(G)$ is initial density matrix and $\mathbf{R}$ is a matrix having elements $R_{KK'}$ given by (8b). Introducing variables

$$\tau=x/u\ ,$$
$$\tau'=\tau-(t-t')\ , \tag{25}$$

one finds that Eq. (24) is reduced to

$$\rho_K(G)=\left\{\exp\left[\mathbf{R}\int_{-\infty}^{\tau}d\tau'\xi_j(1+\cos\{q[z-v(\tau-\tau')]\})\times|f_j(u\tau'-L_j,0)|^2\right]\right\}_{KK'}\rho^i_{K'}(G)\ , \tag{26}$$

which is independent of t. It is also follow from (26) that $\rho_K(G)$ satisfies the differential equations (8), (9), (15) if the replacements

$$t\to\tau, t'\to\tau'\ , \tag{27}$$

are made in these equations. Substituting Eq. (26) in (22) one finds

$$W=3(-1)^{H+G}\hbar\Omega NuS\{H^2G^2\}\begin{Bmatrix}J' & H & I\\ G & J & 1\end{Bmatrix}^2\begin{Bmatrix}1 & 1 & K\\ G & G & H\end{Bmatrix}\times\xi_3\langle[1+\cos(qz+2\varphi_3)]\int_{-\infty}^{\infty}d\tau\epsilon_0^K\rho_K(G)\rangle\ . \tag{28}$$

Equation (8a) is solved subject to the initial condition

$$\rho^i_K(G)=\rho_0(G)\delta_{K0}\ , \tag{29a}$$

where

$$\rho_0(G)=\{GJ^{-2}I^{-2}\}\ . \tag{29b}$$

The interaction with the fields can induce higher multipoles $\rho_K(G)$, where $0\le K\le\hat{K}$ and $\hat{K}$ is an even integer satisfying $2G-1\le\hat{K}\le 2G$. The atomic response differs for open and closed systems, which are treated separately below.

Open transition

An open transition is one in which the excited state can decay to ground-state levels that are decoupled from the fields. The prototype open system is one in which the field drives a $G\to H$ transition and the excited state can decay to a different ground-state hyperfine level $G'\neq G$.

The matrix $R_{KK'}$ has a tridiagonal form

$$R=\begin{bmatrix}R_{00} & R_{02} & 0 & 0 & \dots & 0 & 0 & 0\\ R_{20} & R_{22} & R_{24} & 0 & \dots & 0 & 0 & 0\\ \vdots & \vdots & \vdots & & & \vdots & \vdots & \vdots\\ 0 & 0 & 0 & 0 & \dots & R_{\hat{K}-2,\hat{K}-4} & R_{\hat{K}-2,\hat{K}-2} & R_{\hat{K}-2,\hat{K}}\\ 0 & 0 & 0 & 0 & \dots & 0 & R_{\hat{K},\hat{K}-2} & R_{\hat{K},\hat{K}}\end{bmatrix}\ , \tag{30}$$

and couples multipoles having

$$\Delta K=\pm 2\ . \tag{31}$$

Matrix elements of $\mathbf{R}$, for $J=J'=\frac{1}{2}$, are given in Table I. For open transitions, the matrix $\mathbf{R}$ has negative or zero eigenvalues only, since the field action results asymptotically in optical pumping out of the hyperfine manifold G resonantly coupled to the field, except for those initial sublevels of G for which any excitation on the transition $G\to H$ are forbidden.

Expanding the density matrix in terms of eigenvectors $\mathbf{U}^{(i)}$

$$\rho_K(G)=\alpha_i(\tau)U_K^{(i)}\ , \tag{32}$$

which satisfy the equations $R_{KK'}U^{(i)}_{K'}=-\lambda_i U^{(i)}_K$, where $-\lambda_i$ is eigenvalue i, one finds that the $\alpha_i(\tau)$ satisfy

TABLE I. Values of the matrix R given by (8b), modulus of the eigenvalues λ_i and the eigenvector matrix $\mathcal{U}$ for various nuclear spins I and ground- and first-excited-state total angular momenta G and H, respectively. The data are presented for total ground- and excited-state electronic angular momenta $J=J'=\frac{1}{2}$ only.

I	$G\to H$	R	λ_i	U
	$\frac{1}{2}\to\frac{1}{2}$	(-0.049)	0.049	(1)
	$\frac{1}{2}\to\frac{3}{2}$	(-0.247)	0.247	(1)
1	$\frac{3}{2}\to\frac{1}{2}$	$\begin{pmatrix} -0.025 & 0.025 \\ 0.222 & -0.222 \end{pmatrix}$	0 0.247	$\begin{pmatrix} 0.707 & -0.141 \\ 0.707 & 1.273 \end{pmatrix}$
	$\frac{3}{2}\to\frac{3}{2}$	$\begin{pmatrix} -0.123 & -0.099 \\ -0.198 & -0.247 \end{pmatrix}$	0.032 0.338	$\begin{pmatrix} 0.736 & 0.440 \\ -0.678 & 0.954 \end{pmatrix}$
	$1\to1$	$\begin{pmatrix} -0.069 & -0.049 \\ -0.063 & -0.045 \end{pmatrix}$	0.115 0	$\begin{pmatrix} -0.736 & 0.582 \\ -0.677 & -0.823 \end{pmatrix}$
	$1\to2$	$\begin{pmatrix} -0.208 & 0.029 \\ -0.044 & -0.406 \end{pmatrix}$	0.215 0.399	$\begin{pmatrix} 0.974 & -0.164 \\ -0.225 & 1.064 \end{pmatrix}$
$\frac{3}{2}$	$2\to1$	$\begin{pmatrix} -0.042 & 0.035 & 0 \\ 0.192 & -0.144 & -0.071 \\ 0 & 0.096 & -0.429 \end{pmatrix}$	0 0.215 0.399	$\begin{pmatrix} -0.632 & -0.233 & -0.037 \\ -0.756 & 1.158 & 0.384 \\ -0.169 & 0.520 & 1.265 \end{pmatrix}$
	$2\to2$	$\begin{pmatrix} -0.125 & -0.105 & 0 \\ -0.157 & -0.228 & -0.072 \\ 0 & -0.128 & -0.095 \end{pmatrix}$	0.341 0 0.107	$\begin{pmatrix} 0.395 & 0.448 & -0.521 \\ 0.815 & -0.535 & 0.090 \\ 0.424 & 0.718 & 0.986 \end{pmatrix}$
	$2\to2$	$\begin{pmatrix} -0.086 & -0.072 & 0 \\ -0.083 & -0.120 & -0.038 \\ 0 & -0.049 & -0.036 \end{pmatrix}$	0.190 0.053 0	$\begin{pmatrix} -0.555 & 0.572 & 0.453 \\ -0.793 & 0.264 & -0.542 \\ -0.253 & 0.781 & 0.727 \end{pmatrix}$
	$2\to3$	$\begin{pmatrix} -0.173 & 0.041 & 0 \\ -0.031 & -0.259 & 0.033 \\ 0 & -0.044 & -0.440 \end{pmatrix}$	0.190 0.250 0.432	$\begin{pmatrix} 0.923 & 0.717 & 0.032 \\ -0.380 & -1.347 & -0.201 \\ 0.067 & 0.313 & 1.080 \end{pmatrix}$
$\frac{5}{2}$	$3\to2$	$\begin{pmatrix} -0.062 & 0.043 & 0 & 0 \\ 0.150 & -0.085 & -0.043 & 0 \\ 0 & 0.124 & -0.271 & -0.064 \\ 0 & 0 & 0.062 & -0.455 \end{pmatrix}$	0 0.190 0.250 0.432	$\begin{pmatrix} 0.535 & 0.252 & 0.190 & -0.007 \\ 0.772 & -0.754 & -0.837 & 0.057 \\ 0.342 & -0.970 & -2.568 & 0.441 \\ 0.047 & -0.227 & -0.778 & 1.215 \end{pmatrix}$
	$3\to3$	$\begin{pmatrix} -0.123 & -0.107 & 0 & 0 \\ -0.128 & -0.206 & -0.086 & 0 \\ 0 & -0.119 & -0.186 & -0.057 \\ 0 & 0 & -0.082 & -0.061 \end{pmatrix}$	0.342 0 0.050 0.183	$\begin{pmatrix} 0.343 & -0.378 & -0.447 & 0.457 \\ 0.702 & 0.436 & 0.306 & 0.257 \\ 0.599 & -0.483 & 0.112 & -0.751 \\ 0.175 & 0.658 & -0.903 & -0.504 \end{pmatrix}$
	$3\to3$	$\begin{pmatrix} -0.094 & -0.081 & 0 & 0 \\ -0.088 & -0.141 & -0.059 & 0 \\ 0 & 0.070 & -0.108 & -0.033 \\ 0 & 0 & -0.041 & -0.030 \end{pmatrix}$	0.230 0 0.030 0.114	$\begin{pmatrix} -0.453 & -0.378 & 0.486 & -0.488 \\ -0.758 & 0.436 & -0.381 & -0.121 \\ -0.460 & -0.483 & -0.005 & 0.785 \\ -0.095 & 0.658 & 0.807 & 0.388 \end{pmatrix}$
$\frac{7}{2}$	$3\to4$	$\begin{pmatrix} -0.156 & 0.045 & 0 & 0 \\ -0.116 & -0.198 & 0.050 & 0 \\ 0 & -0.045 & -0.312 & 0.030 \\ 0 & 0 & -0.041 & -0.457 \end{pmatrix}$	0.174 0.202 0.298 0.449	$\begin{pmatrix} -0.923 & -1.586 & -0.198 & -0.007 \\ 0.367 & 1.617 & 0.626 & 0.045 \\ -0.117 & -0.639 & -1.323 & -0.231 \\ 0.017 & 0.104 & 0.344 & 1.104 \end{pmatrix}$
	$4\to3$	$\begin{pmatrix} -0.073 & 0.046 & 0 & 0 & 0 \\ 0.126 & -0.067 & -0.020 & 0 & 0 \\ 0 & 0.120 & -0.185 & -0.062 & 0 \\ 0 & 0 & 0.096 & -0.332 & -0.054 \\ 0 & 0 & 0 & 0.046 & -0.467 \end{pmatrix}$	0 0.174 0.202 0.298 0.449	$\begin{pmatrix} 0.471 & 0.178 & -0.350 & 0.021 & -0.001 \\ 0.752 & -0.395 & 0.991 & -0.105 & 0.006 \\ 0.442 & -0.999 & 4.516 & -1.085 & 0.107 \\ 0.127 & -0.583 & 3.149 & -2.189 & 0.469 \\ 0.012 & -0.091 & 0.545 & -0.595 & 1.201 \end{pmatrix}$

TABLE I *(Continued).*

I	$G\rightarrow H$	R					λ_i	U				
$\frac{7}{2}$	$4\rightarrow 4$	−0.122	−0.107	0	0	0	0.342	0.302	0.391	−0.333	−0.409	−0.411
		−0.118	−0.197	−0.068	0	0	0.226	0.624	0.383	0.380	0.045	0.357
		0	−0.108	−0.190	−0.078	0	0	0.624	−0.396	−0.402	0.502	−0.130
		0	0	−0.101	−0.154	−0.047	0.110	0.353	−0.715	0.449	−0.574	−0.226
		0	0	0	−0.061	−0.044	0.029	0.072	−0.240	−0.617	−0.536	0.888

$$\dot{\alpha}_i(\tau)=-\lambda_i\dot{\varphi}\alpha_i(\tau)\ , \tag{33a}$$

with

$$\varphi=\int_{-\infty}^{t}d\tau'\xi_j[1+\cos(qz_j+2\varphi_j)]|\psi_j(\tau')|^2\ . \tag{33b}$$

Note that φ contains information on the interaction in all three-field zones. The initial conditions are given by

$$\alpha_i(-\infty)=\{J^{-2}I^{-2}G\}(\mathcal{U}^{-1})_{i0}\ , \tag{33c}$$

where the matrix $\mathcal{U}$ is composed of the eigenvectors

$$\mathcal{U}=\begin{bmatrix} U_0^{(0)} & U_0^{(2)} & \cdots & U_0^{(\hat{K})} \\ U_2^{(0)} & U_2^{(2)} & \cdots & U_2^{(\hat{K})} \\ \vdots & \vdots & & \vdots \\ U_{\hat{K}}^{(0)} & U_{\hat{K}}^{(2)} & \cdots & U_{\hat{K}}^{(\hat{K})} \end{bmatrix}\ . \tag{34}$$

Solving Eqs. (33) and substituting $\alpha_i(\tau)$ in (32) and then (28), one obtains

$$W=3(-1)^{H+G}\hbar\Omega NuS\{H^2G^3J^{-2}I^{-2}\}\begin{Bmatrix} J' & H & I \\ G & J & 1 \end{Bmatrix}^2\begin{Bmatrix} 1 & 1 & K \\ G & G & H \end{Bmatrix}$$
$$\times\epsilon_0^K\lambda_i^{-1}\mathcal{U}_{Ki}(\mathcal{U}^{-1})_{iK}\langle\exp(-\lambda_i\{\theta_1[1+\cos(qz_1+2\varphi_2)]+\theta_2[1+\cos(qz_2+2\varphi_2)]\})$$
$$\times(1-\exp\{-\lambda_i\theta_3[1+\cos(qz_3+2\varphi_3)]\})\rangle\ , \tag{35}$$

where

$$\theta_j=2|\varphi_j|^2\Gamma(\gamma^2+\Delta^2)^{-1}\int_{-\infty}^{\infty}\frac{dx}{u}f^2(x,0)\ . \tag{36}$$

We refer to the θ_j's as pulse areas since they play a role for ground-state—ground-state transitions analogous to that played by pulse areas for ground-state—excited-state transitions. Different echolike responses arising from the solution (35) were considered previously [26,27] for arbitrarily polarized pulses in a perturbation-theory limit ($\theta_i\ll 1$). The strong field limit,

$$\theta_i\sim 1\ , \tag{37}$$

is of interest here.

The expression in brackets in (35) oscillates as a function of v and z on scales of order of λ/T and λ, respectively. Conditions (13) and (14) allow one to average over these oscillations before averaging over the particles' distribution function. To carry out the integrations over v and z needed in the average in Eq. (35), one can break up the integrals into domains of order $\Delta v\Delta z$, where

$$\lambda\ll\Delta z\ll b,\lambda/T\ll\Delta v\ll u\theta\ . \tag{38}$$

In each region the distribution function in v and z is approximately constant and can be removed from the integrals. When the contributions from each region are resummed, the result no longer depends on the specific form of the distribution function in v and z. One finds that the expression in brackets in Eq. (35) is equal to

$$\langle\ \rangle=\sum_{n_j}(-1)^{n_1+n_2+n_3}w_{n_1}(\lambda_i\theta_1)w_{n_2}(\lambda_i\theta_2)[\delta_{n_30}-w_{n_3}(\lambda_i\theta_3)]$$
$$\times\int\frac{dz}{\Delta z}\int\frac{dv}{\Delta v}\exp\{iqz(n_1+n_2+n_3)-iqv[n_1T'+n_2(T'-T)]+2i[n_1\varphi_1+n_2\varphi_2+n_3\varphi_3]\}\ , \tag{39}$$

where

$$w_s(x)=e^{-x}I_s(x)\ , \tag{40}$$

and $I_s(x)$ is a modified Bessel function of order s. To arrive at (39) we used a Bessel function expansion for the exponential factors in (35).

The integration over v and z is nonvanishing only if

$$T'/T=L'/L=n_2/(n_1+n_2)\ , \tag{41a}$$

$$n_1+n_2+n_3=0\ . \tag{41b}$$

Thus, one concludes that the ratio of the distances between fields has to be rational. If m and n integers containing no common factors and

$$L'/L=m/n\ , \tag{42}$$

then one finds from Eqs. (41) that the only terms which contribute to the sum (39) are those for which

$$\begin{aligned} n_1&=-(m-n)s\ ,\\ n_2&=ms\ ,\\ n_3&=-ns\ , \end{aligned} \tag{43}$$

where s is an integer. As a consequence for given m and n the absorption can be written as

$$W=\hbar\Omega NuS\sum_{s=0}^{\infty}W_s\cos\{2s[n\varphi_3-m\varphi_2-(n-m)\varphi_1]\}\ , \tag{44a}$$

$$W_s=6(-1)^{H+G}\{H^2G^3J^{-2}I^{-2}\}\begin{Bmatrix}J' & H & I\\ G & J & 1\end{Bmatrix}^2\begin{Bmatrix}1 & 1 & K\\ G & G & H\end{Bmatrix}(\sqrt{\tfrac{1}{3}}\delta_{K0}-\sqrt{\tfrac{2}{3}}\delta_{K2})$$
$$\times\lambda_i^{-1}\mathcal{U}_{Ki}(\mathcal{U}^{-1})_{i0}w_{s(m-n)}(\lambda_i\theta_1)w_{sm}(\lambda_i\theta_2)w_{sn}(\lambda_i\theta_3),\quad s\neq 0\ , \tag{44b}$$

$$W_0=-3(-1)^{H+G}\{H^2G^3J^{-2}I^{-2}\}\begin{Bmatrix}J' & H & I\\ G & J & 1\end{Bmatrix}^2\begin{Bmatrix}1 & 1 & K\\ G & G & H\end{Bmatrix}(\sqrt{\tfrac{1}{3}}\delta_{K0}-\sqrt{\tfrac{2}{3}}\delta_{K2})$$
$$\times\lambda_i^{-1}\mathcal{U}_{Ki}(\mathcal{U}^{-1})_{i0}w_0(\lambda_i\theta_1)w_0(\lambda_i\theta_2)[1-w_0(\lambda_i\theta_3)]\ . \tag{44c}$$

Equations (44) are discussed below.

Closed transition

For a closed transition $G\rightarrow H$, in which the decay $H\rightarrow G'$ of the upper hyperfine sublevel to ground-state sublevels with total angular moment $G'\neq G$ is forbidden by selection rules, the system of equations for the ground-state density-matrix elements becomes linearly dependent, allowing one to decrease the dimension of the matrices **R** and **U**. The final result for the probe absorption takes on a simplified form.

The physical origin of the linear dependence is the conservation of the zeroth multipole of the ground-state density matrix, given by Eq. (29) with $K=0$. Since only $K=0$ and 2 multipoles contribute to the absorption (22) in the case of a linearly polarized fields and since the zero multipole $\rho_0(G)$ is not affected by the field, the shadow effect on the closed transition can appear only owing to the second multipole $\rho_2(G)$. To obtain $\rho_2(G)$ as a solution of Eqs. (8) one separates off terms involving $\rho_0(G)$ and treats them as inhomogeneous driving terms, i.e.,

$$\frac{d}{dt'}\rho_K(G)=\xi_j\{1+\cos[qz(t')+2\varphi_j]\}|\psi_j(t')|^2$$
$$\times[\tilde{R}_{KK'}\rho_{K'}(G)+R_{K0}\rho_0(G)] \tag{45}$$

where $2\leq K\leq\hat{K},2\leq K'\leq\hat{K}$. The matrix $\tilde{R}$ is the dashed part of the matrix (30). Expanding the density matrix in terms of eigenvectors of $\tilde{R}$, $\tilde{\mathbf{U}}^{(2)},\ldots,\tilde{\mathbf{U}}^{(\hat{K})}$, and solving the equations for the coefficients of the expansion, one gets

$$\rho_2(G)=\lambda_i^{-1}\mathcal{U}_{2i}(\mathcal{U}^{-1})_{i2}(1-e^{-\lambda_i\varphi})R_{20}\rho_0(G) \tag{46}$$

where matrix elements of $\mathcal{U}$ are given by

$$\mathcal{U}_{ij}=\tilde{U}_i^{(j)},2\leq i\leq\hat{K},2\leq j\leq\hat{K}\ . \tag{47}$$

Substituting this expression and Eq. (29b) in (28) after integrating over τ one finds

$$W=N\hbar\Omega Su\{H^2G^2J^{-2}I^{-2}\}\begin{Bmatrix}J' & H & I\\ G & J & 1\end{Bmatrix}^2$$
$$\times\left\langle\left[\theta_3+(-1)^{H+G}\sqrt{6}\{G\}\begin{Bmatrix}1 & 1 & 2\\ G & G & H\end{Bmatrix}R_{20}\lambda_i^{-1}\mathcal{U}_{2i}(\mathcal{U}^{-1})_{i2}\right.\right.$$

$$\times[\theta_3-\lambda_i^{-1}\exp(-\lambda_i\{\theta_1[1+\cos(qz_1+2\varphi_2)]+\theta_2[1+\cos(qz_2+2\varphi_2)]\})$$

$$\times(1-\exp\{-\lambda_i\theta_3[1+\cos(qz_3+2\varphi_3)]\})]\Big|\Big\rangle\ . \tag{48}$$

Averaging over v and z as above, one finds the probe-field absorption for closed transitions is given by

$$W=\hbar\Omega NuS\sum_{s=0}^{\infty}W_s\cos\{2s[n\varphi_3-m\varphi_2-(n-m)\varphi_1]\}\ , \tag{49a}$$

where

$$W_s=2\sqrt{6}(-1)^{H+G}\{H^2G^3J^{-2}I^{-2}\}\begin{Bmatrix}J' & H & I\\ G & J & 1\end{Bmatrix}^2\begin{Bmatrix}1 & 1 & 2\\ G & G & H\end{Bmatrix}R_{20}\lambda_i^{-2}\mathcal{U}_{2i}(\mathcal{U}^{-1})_{i2}$$

$$\times w_{s(m-n)}(\lambda_i\theta_i)w_{sm}(\lambda_i\theta_2)w_{sn}(\lambda_i\theta_3),\quad s\neq 0\ , \tag{49b}$$

$$W_0=\{H^2G^2J^{-2}I^{-2}\}\begin{Bmatrix}J' & H & I\\ G & J & I\end{Bmatrix}^2\Big[\theta_3+(-1)^{H+G}\sqrt{6}\{G\}\begin{Bmatrix}1 & 1 & 2\\ G & G & H\end{Bmatrix}R_{20}\lambda_i^{-1}\mathcal{U}_{2i}(\mathcal{U}^{-1})_{i2}$$

$$\times\{\theta_2-\lambda_i^{-1}w_0(\lambda_i\theta_1)w_0(\lambda_i\theta_2)[1-w_0(\lambda_i\theta_3)]\}\Big]\ . \tag{49c}$$

III. DISCUSSION

Equations (44), (49) represent the sought after solutions to the problem for open and closed systems, respectively. The absorption of the third standing wave is expressed as a function of pulse areas θ_j (which depend on the field intensities and atom-field detunings) as well as on the spatial phases φ_j. Since the factor NuS in Eqs. (44a), (49a) gives the total flow of atoms, one can interpret the sums in these equations as the energy absorbed by one atom during its passage through the third-field zone in units of the photon energy $\hbar\Omega$.

The power absorbed from the third field can be used as a measure of the modulation depth of the various gratings contributing to the signal. The signal depends on the phases of the fields through the factor $\cos\{2s[n\varphi_3-m\varphi_2+(m-n)\varphi_1]\}$. If the phase of any of the fields is varied, a Fourier decomposition of the signal yields information on the harmonics that are present in the signal. Harmonic s in the Fourier decomposition, having amplitude W_s, can be associated with the atomic grating having period $\lambda/2sn$, focused in the plane $x=L'$. Moreover, the relative weight of the different Fourier components reflects the relative magnitude of the corresponding atomic gratings.

Before the interaction with the third field, the ground-state Zeeman coherence varies as

$$\exp[2i(n_1+n_2)kz]\exp\{2ikv[n_1T'+n_2(T'-T)]\}$$

$$=\exp(2inskz)\exp[2iskv(nT'-mT)]\ ,$$

where the n_i have to satisfy Eqs. (43). As a consequence, the focusing of the grating having period

$$\lambda_1=\lambda/2n,\quad \lambda_2=\lambda/4n,\quad \lambda_3=\lambda/6n,\ldots, \tag{50}$$

occurs at a distance

$$L'/L=m/n\ . \tag{51}$$

For example, when $m=2$ and $n=1$ ($L'/L=2$), gratings of order $\lambda/2$, $\lambda/4$, $\lambda/6$, etc. are focused. When $m=3$ and $n=2$ ($L'/L=1.5$), gratings of order $\lambda/4$, $\lambda/8$, $\lambda/12$ are focused. For a given n, the lowest order grating is $\lambda/2n$. Each of these gratings is probed by the third field, placed at the appropriate L'. One can interpret the ratio W_s/W_0 as a measure of the modulation depth of the grating having period $\lambda/2sn$.

An aim of this paper is to determine the optimum conditions with respect to the fields and atomic beam parameters for the shadow effect's observation. Let us start from the requirements on the atomic beam. At this stage of our calculations we simplify matters by choosing a monovelocity beam. One can anticipate a decrease of the signal for beams with some distribution over longitudinal velocity u, since the fields' areas θ_j, given by Eq. (36), depend on u, and it is impossible to maintain the same optimal areas simultaneously for atoms with different velocities. In a subsequent paper, we plan to generalize our results for thermal beams and for beams having a narrow velocity distribution in order to determine how large the relative width of the velocity distribution in the beam can be without leading to a significant decrease of the shadow effect signal. The angular divergence of the beam and beam aperture b are taken equal to $\theta=10^{-3}$ rad and $b=0.1$ cm, respectively.

Consider now the requirements for the field parameters. For fields having Gaussian profiles

$$f(x,y)=\exp(-x^2/w_x^2-y^2/w_y^2) \tag{52}$$

the field intensity is related to the field power by

$$P_j=\tfrac{1}{16}cE_j^2w_xw_y\ . \tag{53}$$

From Eq. (36) it then follows that the power is related to the field area θ_j by

$$P_j=(2\pi^5)^{1/2}\frac{\hbar c u w_y}{\lambda^3(2J'+1)}(1+\Delta^2/\gamma^2)\theta_j \tag{54a}$$

or

$$[P_j\ (mW)]=1.009\times10^{-3}\{[T_b(K)/A\}^{1/2}\{\lambda[\mu]\}^{-3}\times(2J'+1)^{-1}[w_y\ (cm)]\times(1+\Delta^2/\gamma^2)\theta_j\ , \tag{54b}$$

where k_BT_b and A are the beam kinetic energy and atomic number, respectively. It is interesting to note that there is no dependence on the transition oscillator strength, i.e., on the matrix element $p_{J'J}$ of the dipole-moment operator appearing in Eqs. (54).

One could have anticipated the result (54) using simple qualitative arguments. Indeed, it is well known that ground-state amplitudes are coupled by terms of order $v_j\sim\chi_j^2/\Delta$, for $|\Delta|\gg\Gamma$. In the resonance case considered here, one has to replace $\Delta\rightarrow\Gamma$, i.e.,

TABLE II. Contribution $\mathcal{W}(l)$ to the third-field's absorption caused by focusing of the atomic grating having period $\lambda/2l$ (harmonic $2l$) in the focal plane $x=L'=[(l+1)/l]L$. [$\mathcal{W}(l)$ represents the contribution per atom in units of the photon energy]. For given values of angular momenta shown, $\mathcal{W}(l)$ is optimized for the ratios of field powers to field aperature w_y given in the last three columns. Only those value of G, H giving an optimum signal are displayed. One can interpret $\mathcal{W}(l)/\mathcal{W}(0)$ as a depth of modulation for the grating having period $\lambda/2l$. The ratio $\mathcal{W}(nl)/\mathcal{W}(l)$ gives the relative contributions of higher-order grating, having period $\lambda/2nl$, at each focal plane L'.

Atom	J'	Transition $G\rightarrow H$	Harmonic $2l$	$\mathcal{W}(l)$	$\frac{\mathcal{W}(l)}{\mathcal{W}(0)}$	$\frac{\mathcal{W}(2l)}{\mathcal{W}(l)}$	$\frac{\mathcal{W}(3l)}{\mathcal{W}(l)}$	P_1/w_y mW/cm	P_2/w_y mW/cm	P_3/w_y mW/cm
Na	$\frac{1}{2}$	$1\rightarrow2$	2	0.008 59	0.257	0.0307	0.0001	0.065	0.192	0.065
			4	0.003 13	0.109	0.0203	0.0001		0.400	0.192
			6	0.001 59	0.068	0.0179	0.0001		0.694	0.400
			8	0.000 96	0.050	0.0170	0.0001		1.072	0.694
			10	0.000 64	0.039	0.0166	0.0001		1.534	1.072
			12	0.000 46	0.032	0.0164	0.0000		2.080	1.534
			14	0.000 35	0.027	0.0163	0.0000		2.710	2.080
			16	0.000 27	0.024	0.0162	0.0000		3.424	2.710
Rb^{85}	$\frac{1}{2}$	$3\rightarrow2$	2	0.010 85	0.258	0.0285	0.0000	0.016	0.048	0.016
			4	0.003 95	0.110	0.0183	0.0002		0.101	0.048
			6	0.002 01	0.069	0.0159	0.0000		0.174	0.101
			8	0.001 21	0.050	0.0151	0.0000		0.270	0.174
			10	0.000 81	0.039	0.0147	0.0000		0.386	0.270
			12	0.000 58	0.032	0.0145	0.0000		0.523	0.386
			14	0.000 44	0.027	0.0144	0.0000		0.682	0.523
			16	0.000 34	0.024	0.0143	0.0000		0.861	0.682
Rb^{85}	$\frac{3}{2}$	$2\rightarrow2$	2	0.00900	0.246	0.0549	0.0048	0.022	0.067	0.022
			4	0.003 29	0.104	0.0440	0.0036		0.138	0.066
			6	0.001 68	0.065	0.0412	0.0032		0.239	0.138
			8	0.001 01	0.047	0.0402	0.0031		0.369	0.239
			10	0.000 68	0.037	0.0398	0.0030		0.528	0.369
			12	0.000 49	0.030	0.0395	0.0030		0.716	0.528
			14	0.000 36	0.026	0.0394	0.0030		0.933	0.716
			16	0.000 28	0.022	0.0393	0.0030		1.179	0.933
Cs	$\frac{1}{2}$	$3\rightarrow4$	2	0.012 12	0.258	0.0292	0.0001	0.010	0.030	0.010
			4	0.004 42	0.110	0.0189	0.0000		0.063	0.030
			6	0.002 25	0.069	0.0166	0.0000		0.109	0.063
			8	0.001 36	0.050	0.0157	0.0000		0.169	0.109
			10	0.000 91	0.039	0.0153	0.0000		0.241	0.169
			12	0.000 65	0.032	0.0151	0.0000		0.327	0.241
			14	0.000 49	0.027	0.0150	0.0000		0.426	0.327
			16	0.000 38	0.024	0.0149	0.0000		0.539	0.426
Cs	$\frac{3}{2}$	$3\rightarrow2$	2	0.012 88	0.519	0.0246	0.0005	0.012	0.036	0.012
			4	0.004 69	0.221	0.0145	0.0005		0.075	0.036
			6	0.002 39	0.139	0.0122	0.0004		0.130	0.075
			8	0.001 44	0.100	0.0114	0.0004		0.201	0.130
			10	0.000 96	0.078	0.0110	0.0004		0.288	0.201
			12	0.000 69	0.064	0.0108	0.0000		0.391	0.288
			14	0.000 52	0.054	0.0107	0.0000		0.509	0.391
			16	0.000 40	0.046	0.0107	0.0000		0.644	0.509

$$\nu_j \sim \chi_j^2/\Gamma \ . \tag{55}$$

Since both χ_j^2 and Γ are proportional to the square of $p_{J'J}$ any dependence on oscillator strength cancels in the rhs of Eqs. (55). Moreover, taking $\theta_j \sim \nu_j w_x/u, \chi_j^2 \sim (p_{J'J}E_j/\hbar)^2 \sim P_j p_{J'J}^2/(c\hbar^2 w_x w_y), \Gamma \sim p_{J'J}^2/[(2J'+1)\hbar\lambda^3]$, and $\Delta=0$, one arrives at Eq. (54a), except for an overall numerical factor.

For a given atomic element, we determine the optimum fields' areas to maximize the contribution to the signal of a given grating. For $\Delta=0$, these quantities can be expressed in terms of the ratio of the field power P_j to field aperture w_y in the direction perpendicular to both and fields and beam propagation directions (see Fig. 3). The results of the calculations are summarized in Table II. Since we are interested in the maximum value of the contribution to the absorption from the grating with period

$$\Lambda=\lambda/2l \ , \tag{56}$$

one needs first to choose the appropriate m and n in the ratio (51). This can be accomplished in the following manner. Even though the absorption (44), (49) contains an infinite set of contributions from the different harmonics, the calculations show that dominant role is played by the first term W_1. From Eqs. (44b), (49b) one concludes that W_1 is larger for smaller values of the indices of the w functions. Since $m > n$, the maximum contribution to the absorption from the grating having period $\lambda/2l$ is found by setting $m=n+1, n=l$, implying that the third field should be located at

$$L'=\frac{l+1}{l}L \ . \tag{57}$$

We set $s=1$, $n=l$, $m=l+1$ in Eqs. (44), (49) and evaluate W_1 as a function of the total angular momenta, G and H, and field areas θ_j. For a given $J \rightarrow J'$ manifold we determine the values of these quantities for which W_1 reaches a maximum. This maximum is denoted $\mathcal{W}(l)$. The contributions to the absorbed power from the grating having spatial period $\lambda/(2sl)$ are denoted $\mathcal{W}(sl)$.

In Table II the results for Na, Rb^{85}, and Cs are presented. The optimum values of the power were calculated for $T_b=300$ K. The absolute value of $\mathcal{W}(l)$ is given in the fifth column. The sixth column contains the ratio $\mathcal{W}(l)/\mathcal{W}(0)$, which can be treated as a modulation depth of the medium, as explained above. The relative amplitudes of the higher harmonics $\mathcal{W}(sl)/\mathcal{W}(l)$ are shown in the columns 7 and 8 for $s=1$ and 2, respectively. The small values of these ratios (not more than 6%), confirms our assumption, that at the distance (57), the grating having period $\lambda/2l$ plays a dominant role under the optimum conditions. The question can be raised as to whether or not a different optimization procedure can result in a reversal of the weights of the various harmonics at a given ratio of L'/L. This does not appear to be the case. For example if the fourth order harmonic rather than the second is optimized for $L'/L=2$, the ratio $W(2)/W(1) \approx 0.2$. This is an increase over the value 0.06 in Table II, but is still less than unity. The optimum values for the ratios P_j/w_y are presented in the last three columns. They were obtained from the optimum fields areas using Eq. (54b).

For alkali-metal atoms such as K and Rb^{87} which have the same nuclear spin $I=\frac{3}{2}$ as Na, one needs only to change the data for P_j/w_y by factors of 0.344 and 0.209 for K and Rb, respectively, if the excited-state angular momentum is $J'=\frac{1}{2}$, and by factors 0.35 and 0.222 for $J'=\frac{3}{2}$. Results for the D_2 line of Na are omitted since they coincide with those for the D_1 line. This coincidence is caused by the fact that, for both values of the excited-state electronic angular moment, the optimum hyperfine component of the manifold is the $G=1 \rightarrow H=2$ transition. For this particular transition, the matrix R for the D_1 line and its eigenvalues are twice as larger as those for D_2 line, while the eigenvectors $\mathbf{U}^{(i)}$ coincide. As a consequence, the optimum fields areas for the D_1 line are half as small as those for the D_2 line, but this difference is canceled by the factors $(2J'+1)^{-1}$ in Eqs. (54) when one calculates the optimum powers.

The optimum power P_1 for the first field is the same for all transitions. Moreover, the optimum power of the second-field power P_2 for grating $2l$ coincides with the optimum value of the third-field power P_3 for grating $2(l+1)$. This result would suggest that the expression of W_1 factors as

$$W_1=F_1(\theta_1)F_{l+1}(\theta_2)F_l(\theta_3) \ . \tag{58}$$

In fact, this expression can be derived from previous results on the shadow effect [3] in two-level systems whose levels are not coupled by spontaneous decay. We checked the validity of Eq. (58) and found that it does not hold in the whole three-dimensional space of the fields' areas $(\theta_1, \theta_2, \theta_3)$, but was approximately correct in some vicinity of the optimum points.

As an application, consider the D line in Na $\lambda=0.59\mu$, for a Na beam having angular divergence $\theta=10^{-3}$, aperture $b=0.1$ cm and velocity $u=5\times10^4$ cm/s. For such a beam to participate entirely in the shadow effect, conditions (12) and (14) must hold. Condition (14) $(b/w_y \ll 1)$ ensures that entire beam in the y direction is illuminated by the field. (Corrections to Eq. (36) can be shown to be of order $\exp[-2(b/w_y)^2]$.) On the other hand, condition (12) $(kw_x\theta \ll 1)$ ensures that all velocity groups are excited by the field. [Corrections to the arguments of the Bessel functions in Eq. (40) can be shown to be of order $\exp[-(k\theta w_x)^2]$. We choose $w_y=0.4$ cm and $w_x=30\mu$ for which $\exp[-2(b/w_y)^2] \approx 0.88$ and $\exp[-(k\theta w_x)^2] \approx 0.91$. For this value of w_y, the optimum fields powers are in the range $0.026 \text{ mW} \le P_j \le 1.37$ mW and the modulation depth changes from 26% for the second-order grating with period 0.3μ to 2.4% for 16th order grating with period 37 nm.

ACKNOWLEDGMENTS

We are happy to acknowledge helpful discussions with T. Sleator, A. Kumarakrishnan, I. Barkan, and S. Cahn in the NYU. This work is supported by the U.S. Army Research Office, by the National Science Foundation through the Center for Ultrafast Optical Science under Grant Nos. STC PHY 8920108 and PHY 9396245.

[1] A review of laser cooling below the Doppler limit including an extensive bibliography can be found in P. D. Lett, W. D. Phillips, S. L. Rolston, C. E. Tanner, R. N. Watts, and C. I. Westbrook, J. Opt. Soc. Am. B **6**, 2084 (1989); J. Dalibard and C. Cohen-Tannoudji, *ibid.* **6**, 2023 (1989); P. J. Ungar, D. S. Weiss, E. Riis, and S. Chu, *ibid.* **6**, 2058 (1989); D. S. Weiss, E. Riis, Y. Shevy, P. J. Ungar, and S. Chu, *ibid.* **6**, 2072 (1989); A. Aspect, E. Arimondo, R. Kaiser, N. Vanteenkiste, and C. Cohen-Tannoudji, *ibid.* **6**, 2112 (1989).

[2] B. Ya. Dubetsky, A. P. Kasantsev, V. P. Chebotayev, and V. P. Yakovlev, Pis'ma Zh. Eksp. Teor. Fiz. **39**, 531 (1984) [JETP Lett. **39**, 649 (1984)]; Zh. Eksp. Teor. Fiz. **89**, 1190 (1985) [Sov. Phys. JETP **62**, 685 (1985)].

[3] V. P. Chebotayev, B. Ya. Dubetsky, A. P. Kasantsev, and V. P. Yakovlev, J. Opt. Soc. Am. B **2**, 1791 (1985).

[4] R. Friedberg and S. R. Hartman, Phys. Rev. A **48**, 1446 (1993).

[5] R. Friedberg and S. R. Hartman, Laser Phys. **3**, 526 (1993).

[6] M. Prentiss, G. Timp, N. Bigelow, R. E. Behringer, and J. E. Cunningham, Appl. Phys. Lett. **60**, 1027 (1992).

[7] T. Sleator, T. Pfau, V. Balykin, J. Mlynek, Appl. Phys. B **54**, 375 (1992).

[8] G. Timp, R. E. Behringer, D. M. Tennant, J. E. Cunningham, M. Prentiss, and K. Berggren, Phys. Rev. Lett. **69**, 1636 (1992).

[9] V. P. Chebotayev (unpublished).

[10] J. F. Clauser and M. W. Reinsch, Appl. Phys. B **54**, 380 (1992).

[11] D. W. Keith, C. R. Ekstrom, Q. A. Turchette, and D. E. Pritchard, Phys Rev. Lett. **66**, 2693 (1991).

[12] T. Mossberg, R. Kachru, E. Whittaker, and S. R. Hartman, Phys. Rev. Lett. **43**, 851 (1979).

[13] B. Ya. Dubetsky and V. M. Semibalamut, Kvant. Elektron. **9**, 1688 (1982) [Sov. J. Quantum Electron. **12**, 1081 (1980)].

[14] See, for example, P. R. Berman, D. G. Steel, G. Khitrova, and J. Liu, Phys. Rev. A **38**, 252 (1988).

[15] P. R. Berman, Phys. Rev. A **43**, 1470 (1991).

[16] P. R. Berman, Phys. Rev. A **49**, 2922 (1994).

[17] G. Rogers, and P. R. Berman, Phys. Rev. A **50**, 611 (1994).

[18] A. P. Kol'chenko, S. G. Rautian, and R. I. Sokolovskii, Zh. Eksp. Teor. Fiz. **55**, 1864 (1968) [Sov. Phys. JETP **55**, 986 (1968)].

[19] J. L. Hall, C. Borde, and K. Uehara, Phys. Rev. Lett. **37**, 1339 (1976).

[20] B. Ya. Dubetsky and V. M. Semibalamut, in *Sixth International Conference on Atomic Physics Abstracts,* edited by E. Anderson, E. Kraulineya, and R. Peterkop (Riga, USSR, 1978), p. 21.

[21] J. C. Bergquist, R. L. Barger, and D. J. Glase, Appl. Phys. Lett. **34**, 850 (1979).

[22] D. S. Weiss, B. C. Young, and S. Chu, Phys. Rev. Lett. **70**, 2706 (1993).

[23] J. Guo, P. R. Berman, B. Dubetsky, and G. Grynberg, Phys. Rev. A **46**, 1426 (1992).

[24] J. Y. Courtois, G. Grynberg, B. Lounis, and P. Verkerk, Phys. Rev. Lett. **72**, 3017 (1994).

[25] P. R. Berman, G. Rogers, and B. Dubetsky, Phys. Rev. A **48**, 1506 (1993).

[26] B. Dubetsky and P. R. Berman (unpublished).

[27] B. Dubetsky, P. R. Berman, and T. Sleator, Phys. Rev. A **46**, 2213 (1992); B. Dubetsky and P. R. Berman (unpublished).

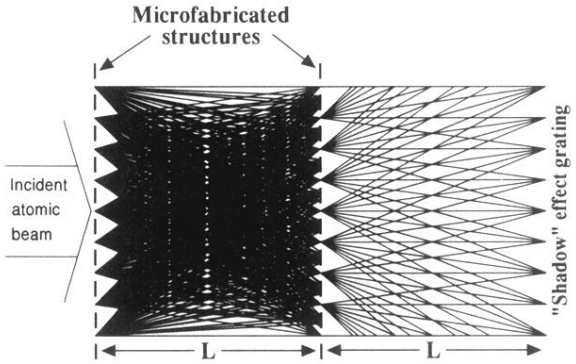

FIG. 1. "Shadow" effect. Microfabricated structures with period d simulate action of separated standing waves with wavelength $\lambda=2d$. An atomic density grating, i.e., a periodical spatial distribution with period $\lambda/2$, appears just after the first structure. Overlapping of the trajectories of atoms passing through the different slits results in the rapid destruction of the grating in a distance λ/θ. An atomic beam with angular divergence $\theta\sim 1$ is assumed here. The trajectories of the particles passing through the centers of slits are shown after the second microfabricated structure. Superposition of the "shadows" from the first and second structures leads to grating reconstruction exactly at the distance $2L$.

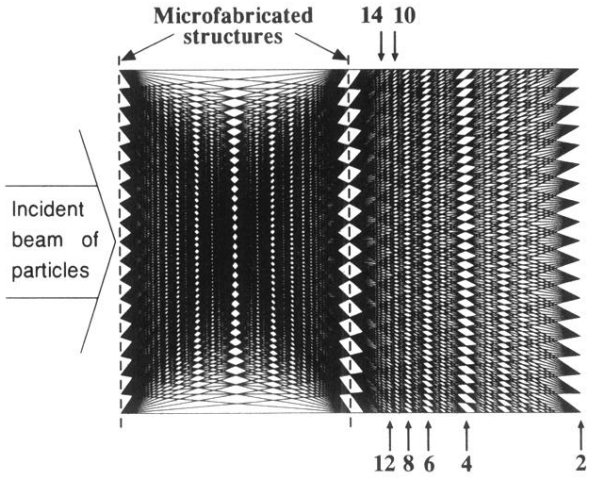

FIG. 2. "Shadow" effect using two microfabricated structures of 20 slits each; n th arrow shows point of localization for harmonic n. The gratings appearing at distance between the structures are washed out by trajectories (not shown) which do not pass through the second set of slits.